ADVANCED OPTICAL MATERIALS

Supporting Information

for *Adv. Optical Mater.,* DOI: 10.1002/adom.202100620

Perovskite Quantum Dots for Super-Resolution Optical Microscopy: Where Strong Photoluminescence Blinking Matters

Leon G. Feld, Yevhen Shynkarenko, Franziska Krieg, Gabriele Rainò, and Maksym V. Kovalenko**

Supporting Information

Perovskite Quantum Dots for Super-resolution Optical Microscopy: where Strong Photoluminescence Blinking Matters

Leon G. Feld, Yevhen Shynkarenko, Franziska Krieg, Gabriele Rainò, Maksym V. Kovalenko**

Institute of Inorganic Chemistry, Department of Chemistry and Applied Biosciences, ETH Zurich,8093 Zurich, Switzerland

Laboratory for Thin Films and Photovoltaics, Empa − Swiss Federal Laboratories for Materials Science and Technology, 8600 Dübendorf, Switzerland

* corresponding authors: rainog@ethz.ch, mvkovalenko@ethz.ch

1. Synthesis and sample preparation

1.1. Synthesis and characterization of $CsPbBr_3$ Nanocrystals

The solution phase synthesis of ASC18-capped $CsPbBr_3$nanocrystals (NCs) was carried out according to the procedure reported before.[1] A typical procedure to prepare the reactants and product is described below.

1.1.1. Cs-oleate 0.4 M in 1-octadecene (ODE)

Cesium carbonate (1.628 g, 10 mmol; FLUOROCHEM), oleic acid (5 mL, 16 mmol; SIGMA ALDRICH/MERCK), and 1-octadecene (20 mL; technical grade; SIGMA ALDRICH/MERCK) were evacuated at 25-120°C until gas formation was complete.

Pb-Oleate 0.5 M in ODE: Lead (II) acetate trihydrate (4.6 g, 12 mmol; SIGMA ALDRICH/MERCK), oleic acid (7.6 mL, 24 mmol) and 1-octadecene (16.4 mL) were added to a three necked flask and evacuated at 25-120°C until acetic acid and water have evaporated.

1.1.2. TOP-$Br_2$0.45 M in mesitylene

Under argon atmosphere, trioctylphosphine (TOP; 6 mL, 13 mmol; >97%, STREM) and Bromine (0.6 mL, 11.5 mmol; SIGMA ALDRICH/MERCK) were mixed. After the exothermic reaction finished, the mixture was allowed to cool to room temperature and TOP-Br_2 was dissolved in mesitylene (18.7 mL; SIGMA ALDRICH/MERCK).

1.1.3. ASC18-capped $CsPbBr_3$ NCs

Pb-oleate (0.5 mL, 0.25 mmol), cesium oleate (0.4 mL, 0.16 mmol) and ASC18 (0.0222 g) were dissolved in 5 mL ODE under vacuum and under heating to 130°C. Under Argon atmosphere, the precursor solution was further heated to 180°C and TOP-Br_2 (0.5 mL, 0.75 mmol) was injected. The reaction mixture was quickly cooled down to room temperature with an ice bath. The crude solution was centrifuged (29464 g, 10 min, 17°C). The precipitate was redispersed in 3 mL of toluene and again centrifuged (29464 g, 10 min, 17°C) to remove impurities. The residual solution was used for sample preparation and characterization.

1.1.4. Characterization

The ASC18-capped $CsPbBr_3$ NCs, prepared as described above, were characterized by Photoluminescence (PL) spectroscopy and Transmission Electron Microscopy (TEM). The absorption and emission spectra, as well as TEM images, are shown in **Figure S1**. PLPeak

position and full-width at half maximum (FWHM), PL quantum yield (QY) and the approximate particle size determined by TEM are listed in the **Figure S1** caption.

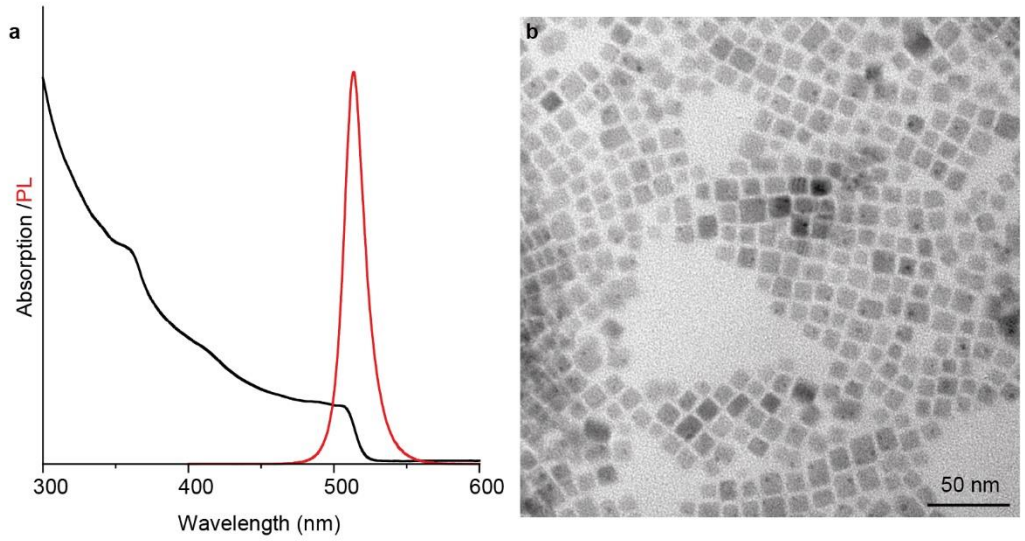

Figure S1. Characterization of ASC18-capped $CsPbBr_3$ NCs. a) Absorption (black line) and emission (red line) spectra of a colloidal solution of ASC18-capped $CsPbBr_3$ NCs. The PL peak is at a wavelength of 514 nm and features a FWHM of 19 nm. A PLQY of 75% was determined. b) TEM images of ASC18-capped $CsPbBr_3$ NCs. The average particle size obtained from TEM is 9.6 ± 1.5 nm

1.2. Sample preparation for optical measurements

A polystyrene film doped with $CsPbBr_3$ NCs was prepared by spin-coating on a glass substrate according to the following procedure.A 3.5 mg/mL solution of $CsPbBr_3$ NCs in dry toluene, prepared according to the procedure above, was diluted 100-fold with dry toluene. 10 µL of this solution were diluted in 1600 µL dry toluene and 400 µL of a 5% solution of polystyrene in dry toluene. Of the obtained NC/polystyrene solution, 100 µL were spin-coated under laminar flow on a thin glass substrate (coverslip; thickness 170 ± 5 µm; diameter 25 mm; from Thorlabs) at 3000 rpm for 60 seconds.

2. Optical measurements

2.1. Single-emitter spectroscopy

A home-built setup for single-emitter spectroscopy was used, which is composed of a pulsed Picoquantlaser (10 MHz repetition rate,< 50 ps pulses, < 100 W/cm^2, 405 nm), which is focused (1/e^2=1 μm) by an oil immersion objective (NA=1.3). The emitted light is passed through the same objective and a dichroic filter to eliminate contributions from the excitation laser. The emitted light is either analysed by a Hanbury-Brown and Twiss (HBT) setup with a 50/50 beam splitter, two APDs (temporal resolution=250 ps) and a correlation card or by a monochromator and EMCCD camera (binning time 1 s).For wide-field microscopy, the same home-built setup was used withan additional lens which focuses the laser on the back focal plane of the objective, thus widening the spot area on the sample. The PL image is then recorded by the same oil immersion objective and EMCCD camera (binning time 0.3 s).Using an absorption cross section of 2 e-14 cm^2,[2]the average number of absorbed photons is estimated to be 0.02 (4.4 W/cm^2 irradiance, 0.4 μJ/cm^{2}excitation fluence). For single-molecule localization microscopy (SMLM), a video with 500 frames at a binning time of 0.3 s was recorded.

3. Data analysis

Data analysis was carried out in MATLAB using open source tools, which are referred to below.

3.1. Localization

A video of blinking quantum dots(QDs) with 500 frames and binning time of 0.3 s was corrected for stage drift and candidate positions were identified (iSMS[3]). To each frame of the candidate spot a rotated elliptical 2D Gaussian was fitted (psfFit from the TrackNTraceframework[4]) and low intensity frames (three times the standard deviation of noise) were removed. The intensity and ellipticity time traces were obtained from the parameters of the fit.

3.2. Intensity filtering

Intensity filtering was carried out as proposed in previous work.[5-6] However, we have struggled finding distinct levels in the traces as discussed in the main text and as it is apparent in **Figure S2**.

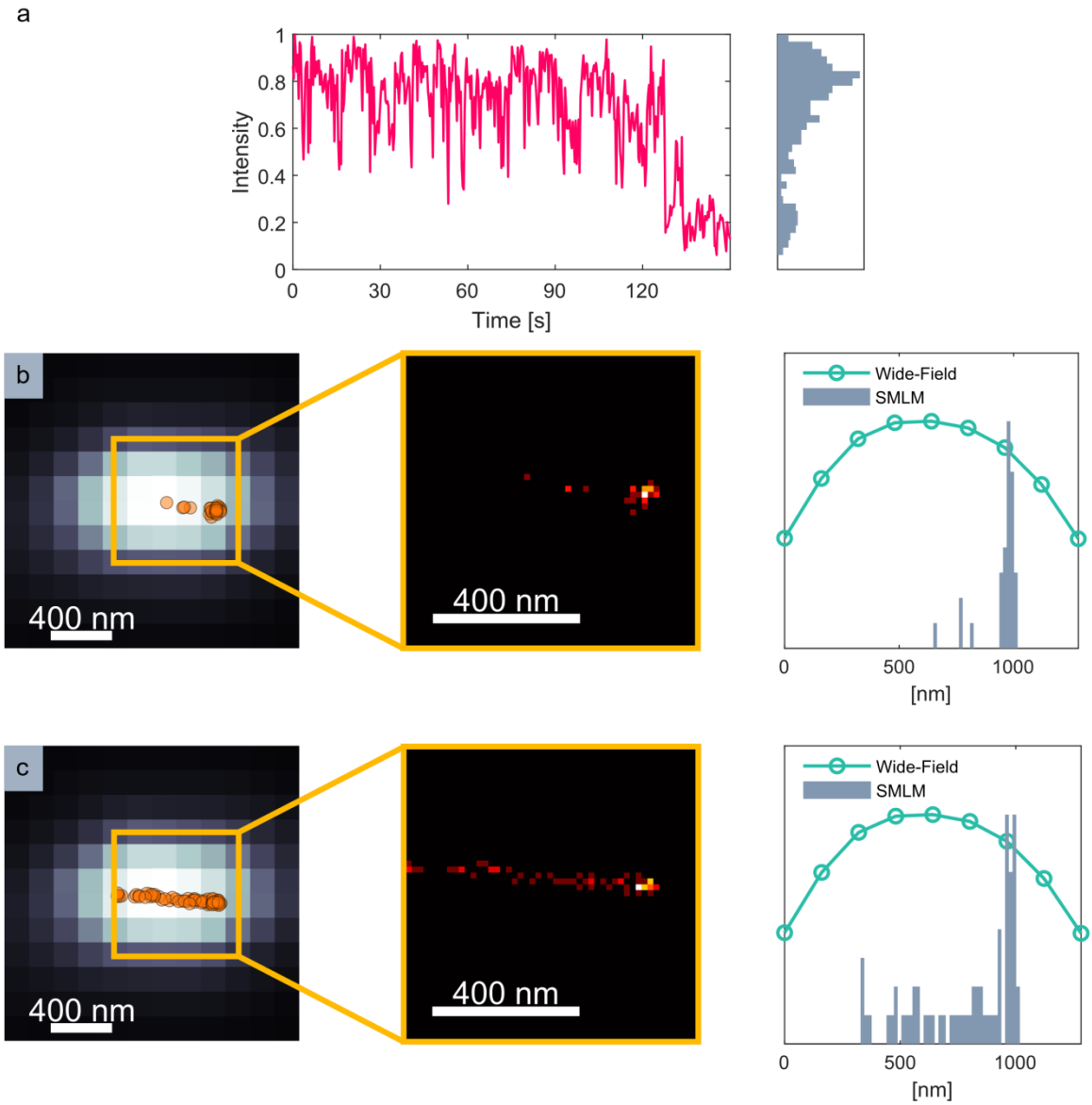

Figure S2. Intensity filtering for two nearby emitters. a) Trace of the bright spot and corresponding histogram of the intensities. Three distinct levels could not be found. b-c) dSTORM images of the intensity ranges 0-0.2 (b) and 0.2-0.5 (c) are shown. On the left, the

wide-field image (bright pixels) and localizations (orange dots) are shown. In the centre, histograms of the enlarged area are shown. Profiles of the wide-field image (green line and circles) and histograms of the localizations with intensities within the ranges (grey bars) are shown on the right. Comparing this to **Figure 2** from the main text, we do not recover the true position of the left emitter by intensity filtering.

3.3.Ellipticity Filtering

Ellipticity filtering is described in the main text for one example (**Figure 2**). In **Figure S3**, the procedure to obtain the threshold value is highlighted. To identify the optimal threshold, we reduced the ellipticity threshold until the positions of localizations remains unaltered (see **Figure S3**). Further decreasing the threshold only reduces the number of localizations at the emitterpositions.

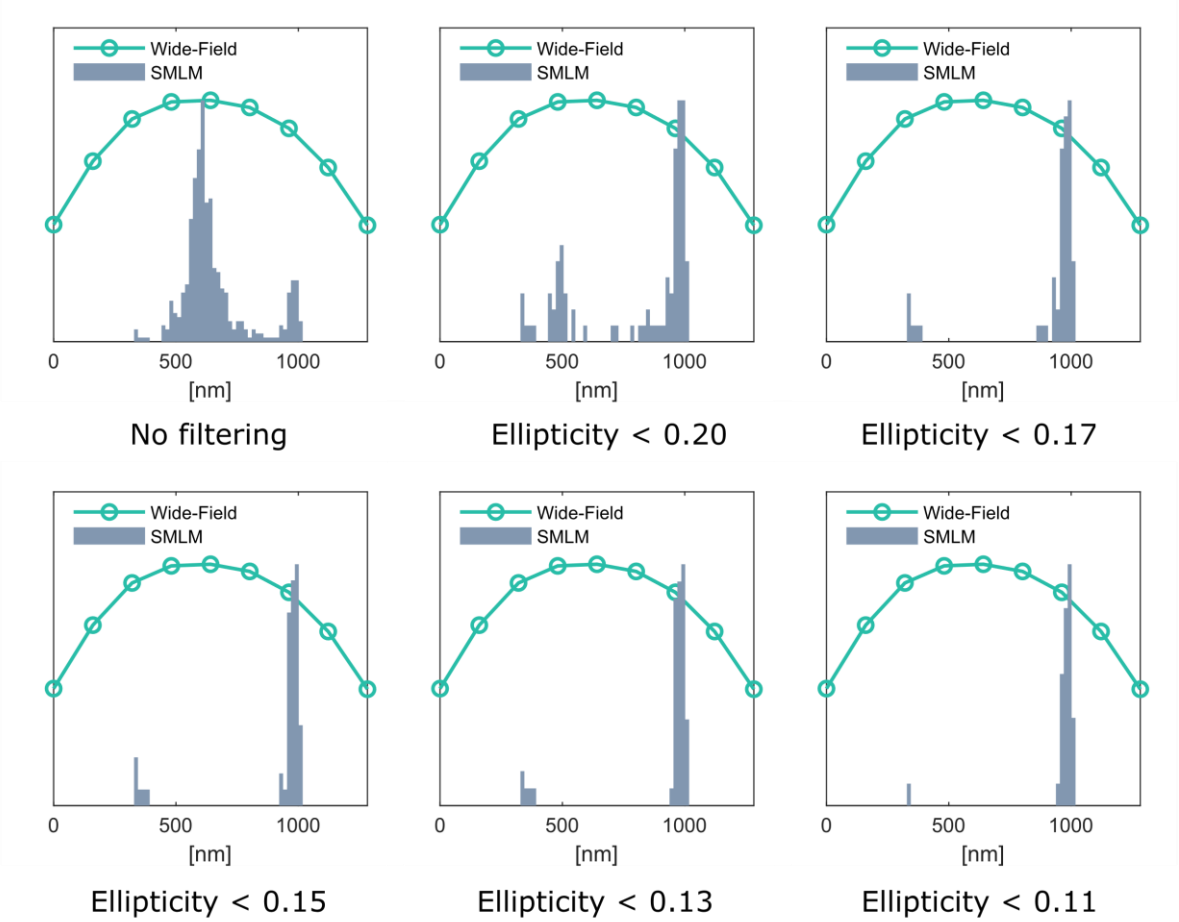

Figure S3. Choosing the ellipticity threshold. Reducing the ellipticity threshold to 0.15 removes false localizations. Reducing the threshold further does not change the positions of localizations, but reduces the number of localizations.

More examples of ellipticity filtering are shown below in **Figure S4.** Here, the same ellipticity threshold as in the example in the main text (0.15) is used.

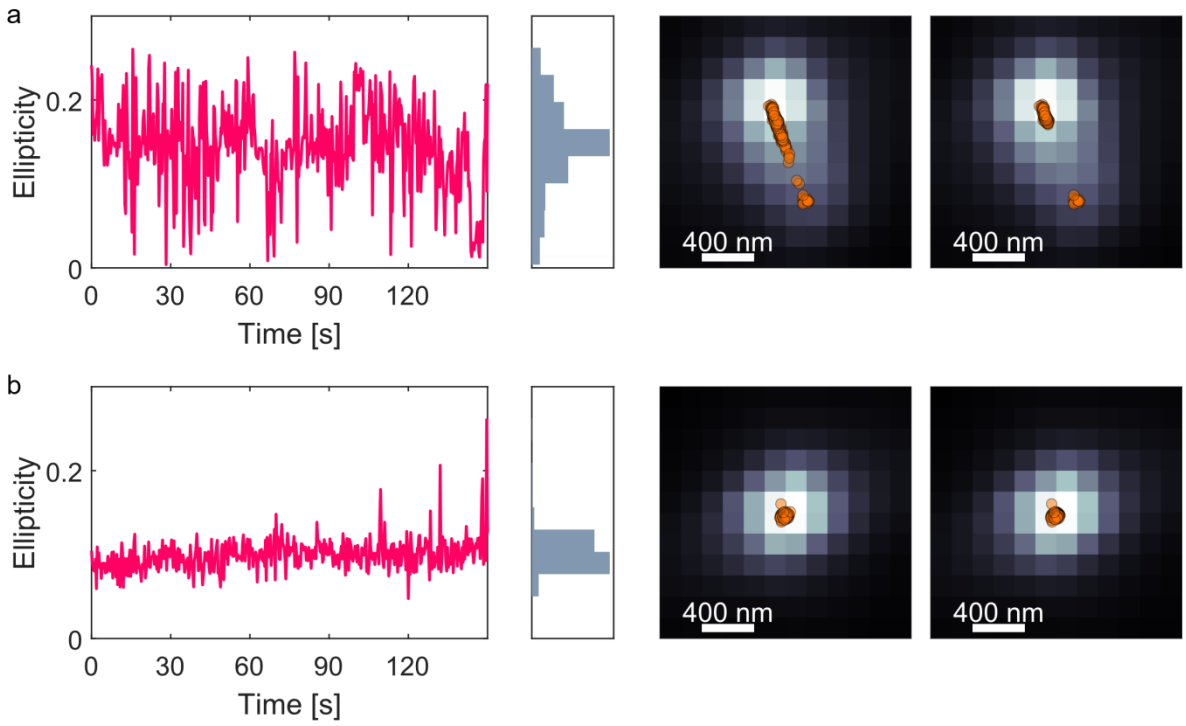

Figure S4. More examples of ellipticity filtering. For each spot, the ellipticity trace with histogram (red line, grey bars), the SMLM analysis without filtering (left image) and with a threshold of 0.15 (right image) is shown. In the images, the confocal image (bright pixels) and the localizations with ellipticities below threshold (orange points) are shown. a) This example shows an ellipticity trace with distinct levels and we can observe improved positions after filtering. b) Ellipticity filtering of an isolated QD as shown in**Figure 1**of the main text. In this case ellipticity remains below the threshold value of 0.15 used for discriminating closely spaced QDs.

4. Simulations

4.1 Absorption cross-section and Localization precision

This section describes how the expression for **Figure 3**f from the main text is obtained, which is then used for simulations in **Figure 3**b-e, as well as **Figure 3**h. The starting point is the well-known relation for the localization error

$$\Delta \propto \frac{1}{\sqrt{m}} \ ,$$

where m is the number of photons collected for the localization.[7] Assuming photoexcitation in the linear regime, *i.e.* photon absorption is not life-time limited due to saturation, the number of collected photons is proportional to the absorption cross section σ_{abs} and excitation intensity I:

$$\Delta \propto \frac{1}{\sqrt{\sigma_{abs} \times PLQY}}. \qquad (1)$$

Using expression (1), we obtain the localization precision for a material with an absorption cross-section σ_{abs} from a reference material with Δ_{ref} and $\sigma_{abs,ref}$ as

$$\Delta(\sigma_{abs}) = \Delta_{ref} \sqrt{\frac{\sigma_{abs,ref}}{\sigma_{abs}}} \ , \qquad (2)$$

where we additionally assumed similar PLQY and unchanged experimental conditions.This equation is plotted in **Figure 3**f of the main text.

As a reference, the organic dye AlexaFluor647 (AF647) was chosen due to its popularity and availability of data.[8]All parameters for **Figure 3**b-hare listed in**Table S1** below.

Table S1. Reference values for **Figure 3**b-h from the main text.

Parameter	Value	Source
Δ_{ref}	10 nm	[8]
Binning Time	33.3 ms	[8]
$\sigma_{abs,ref} = \sigma_{abs,AF647}$	9.1 e-16 cm^2	[8]
r_{AF647}	0.0005	[8]
PLQY$_{AF647}$	0.33	[8]
$\sigma_{abs,CsPbBr_3}$	2.0 e-14 cm^2	[2]

$PLQY_{CsPbBr3}$	0.5	This work

4.2 Simulating SMLM images

To simulate the SMLM images from **Figure 3**b-e, we chose a Monte-Carlo approach based on the ON/OFF ratiosof the emitters. In a diffraction limited spot with K emitters (e.g. 5-by-5 emitters, 50 nm separation) each emitter and frame are treated independently assuming QD that blinking can be described as a Morkov process (memoryless) and that the states of QDs are independent variables (non-interacting). The probability of a frame being dark (all emitters are in OFF-state), useful (exactly one emitter is ON), or false localization (multiple emitters are ON) is then described by a binomial distribution, where the probability of single emitter being in itsON-state is equal to the ON/OFF ratio$r$. The binomial distribution of a grid with K emitters describes the probability of n_{on} emitters being in their ON-state simultaneously:

$$P_{n_{on}} = \binom{K}{n_{on}} r^{n_{on}} (1-r)^{K-n_{on}} \tag{3}$$

Frames, in which only a single emitter is ON, are useful frames for SMLM.The fraction of useful frames is

$$P_{useful} = P_1 = \binom{K}{1} r(1-r)^{K-1} \tag{4}$$

and for a total number of framesN_{tot} we obtained the number of useful localizations

$$N_{useful} = N_{tot} \binom{K}{1} r(1-r)^{K-1} \quad . \tag{5}$$

The number of localizations per emitter is

$$N_{loc} = \frac{N_{tot}}{K} \binom{K}{1} r(1-r)^{K-1} \quad . \tag{6}$$

Analogously, we can find the number of dark frames

$$N_{dark} = N_{tot} P_{n=0} = N_{tot} \binom{K}{0} (1-r)^K$$

The number of false localizations, which occur if multiple emitters are on simultaneously is

$$N_{false} = N_{tot} - N_{useful} - N_{dark}$$

$$= N_{tot} P_{n>1} = N_{tot} \sum_{n_{on}=2}^{K} \binom{K}{n_{on}} r^{n_{on}} (1-r)^{K-n_{on}} \quad . \tag{7}$$

In **Figure 3**g, the fraction of false localizations as well as dark and useful frames are plotted based on Equation 3, 4 and 7.

With the derived numbers of localizations per emitter, false localizations and dark frames for a given number of frames, we can generate the images in **Figure 3**b-e. The position of useful localizations are described by a normal distribution defined by the localization error Δ around the position of the respective emitter. To generate an image, we draw for each emitter N_{loc} points from this distribution. Positions of false localizations are then drawn from an elliptical normal distribution around the mean position of all emitters, that are ON. The covariance matrix of this distribution is chosen as Σ, where Σ is the covariance of the positions of emitters, which are in ON-states. For dark frames, no localizations are added to the image.

4.3 Minimum Number of Frames

For **Figure 3**h of the main text, we combine the equation for the root-mean-square error (RMSE) of the mean of localizations

$$RMSE = \frac{\Delta}{\sqrt{N_{useful}}} = \frac{\Delta}{\sqrt{N_{tot} \times \binom{K}{1} r\,(1-r)^{K-1} K^{-1}}} \quad , \tag{8}$$

which was derived in the main text, with Equation 2. We obtain the minimum number of frames required for a fixed RMSE for different absorption cross sections σ_{abs} and ON/OFF ratios:

$$N_{tot}(\sigma_{abs}, r) = \frac{\sigma_{abs,ref}}{RMSE^2 \times \sigma_{abs} \times \Delta_{ref}{}^2 \times r\,(1-r)^{K-1}} \quad (9)$$

Here, we assumed that the distributions of localizations of different emitters are separable. Additionally, we assume complete suppression of false localizations. The RMSE does not correspond to an emitter's resolution limit, which is still limited by the localization error, but it does give a good idea of the image quality, including the signal-to-noise ratio. For **Figure 3**h RMSE is chosen as 1 nm.

References

[1] F. Krieg, S. T. Ochsenbein, S. Yakunin, S. Ten Brinck, P. Aellen, A. Süess, B. Clerc, D. Guggisberg, O. Nazarenko, Y. Shynkarenko, S. Kumar, C. J. Shih, I. Infante, M. V. Kovalenko, *ACS Energy Lett.***2018**, 3, 641.

[2] N. A. Gibson, B. A. Koscher, A. P. Alivisatos, S. R. Leone, *J. Phys. Chem. C***2018**, 122, 12106.

[3] S. Preus, S. L. Noer, L. L. Hildebrandt, D. Gudnason, V. Birkedal, *Nat. Methods***2015**, 12, 593.

[4] S. C. Stein, J. Thiart, *Sci. Rep.***2016**, 6, 37947.

[5] F. C. Chien, C. W. Kuo, P. Chen, *Analyst***2011**, 136, 1608.

[6] B. C. Lagerholm, L. Averett, G. E. Weinreb, K. Jacobson, N. L. Thompson, *Biophys. J.***2006**, 91, 3050.

[7] R. E. Thompson, D. R. Larson, W. W. Webb, *Biophys. J.***2002**, 82, 2775.

[8] G. T. Dempsey, J. C. Vaughan, K. H. Chen, M. Bates, X. Zhuang, *Nat. Methods***2011**, 8, 1027.